Improvement of bias current subtraction for Himawari-8/SEDA-e observation

T. Nagatsuma and K. Sakaguchi

Space Environment Laboratory, Radio Research Institute, National Institute of Information and Communications Technology

GSICS Annual Meeting GRWG SWx sub-group session
4e Tuesday, 12 Mar. 2024, 10:10-10:25

Space Environment Data Acquisition Monitor (SEDA) onboard Himawari-8,9

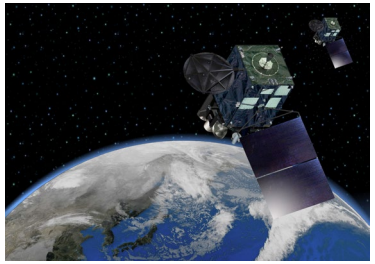

Items	Description
Number of Channels	Protons : 8 (individual 8 sensor elements) Electrons : 8 (8 stacked plates in one elements)
Energy Range	Protons : 20 MeV – 100 MeV Electrons : 0.2 MeV – 5 MeV
Time Resolution	10 sec.
Field of View	Protons : ± 39.35 deg. Electrons : ± 78.3 deg.

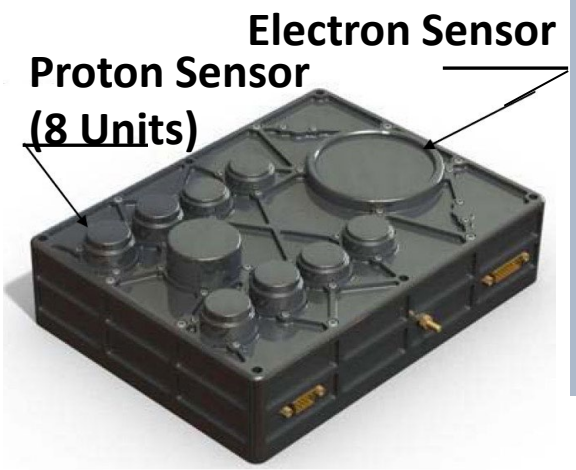

- High-energy particle environment over Japanese sector has been monitored by SEDA since Nov. 03, 2014.
- Near-real time SEDA data is provided from JMA to NICT. We have been using SEDA data for space weather forecast, and providing SEDA data as part of space weather information.

Longitude: ~140 deg.
Himawari-8 Launch: 2014/10/07
Himawari-9 Launch: 2016/11/02

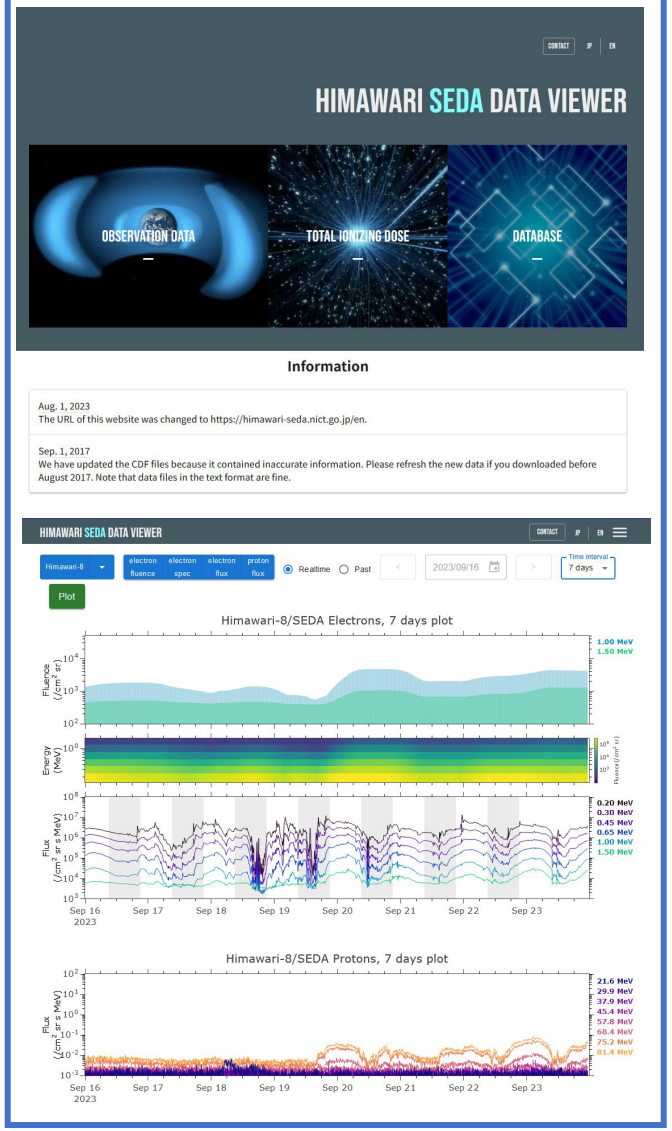

https://himawari-seda.nict.go.jp

SEDA-e

Ch0: 0.2 MeV
Ch1: 0.3 MeV
Ch2: 0.45 MeV
Ch3: 0.65 MeV
Ch4: 1.0 MeV
Ch5: 1.5 MeV
Ch6: 2.0 MeV
Ch7: 4.5 MeV

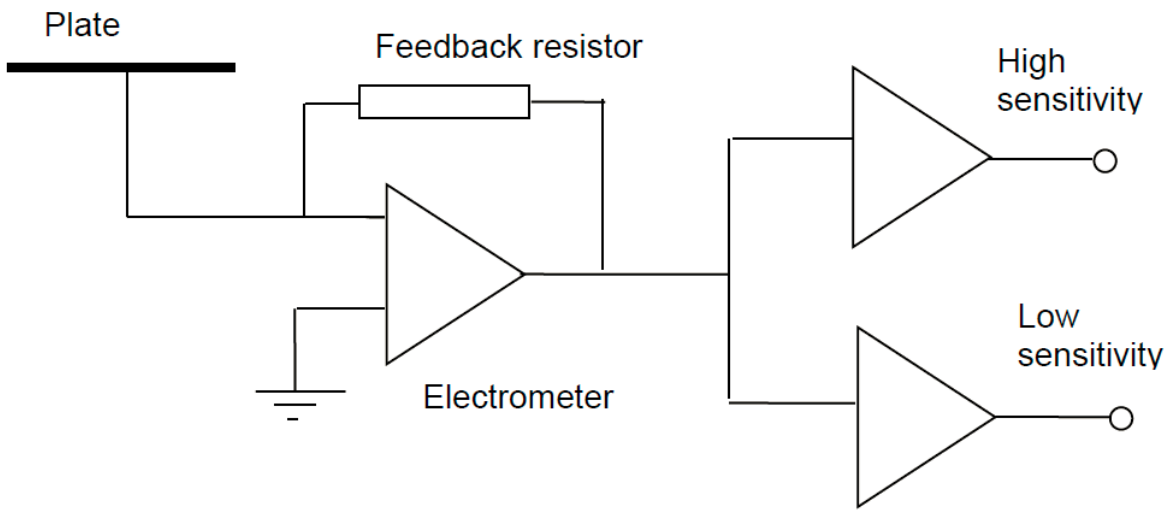

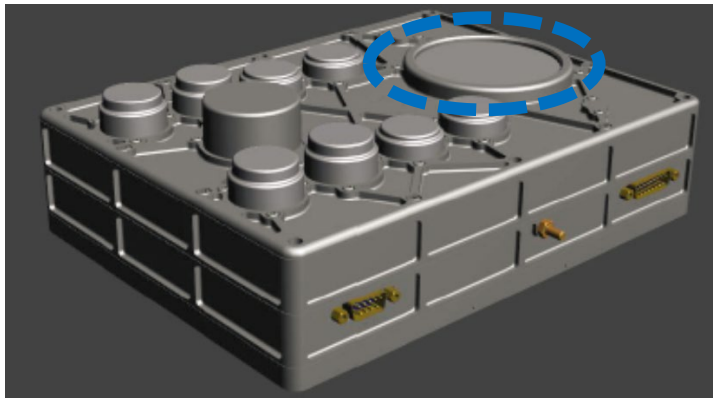

- SEDA-e measures internal charging currents produced from high energy electrons (0.2 – 4.5 MeV) collected by 8 plates arranged in a stack. Electron fluxes are estimated from the charging currents.
- Since a bias current is added to the measured current (voltage) by an operational amplifier, estimation of electron flux requires subtraction of the bias current.
- Bias current is a function of sensor temperature. A model function is estimated based on ground experiments.

Long-term variations of SEDA-e measurements (2015-2021) all Ch.

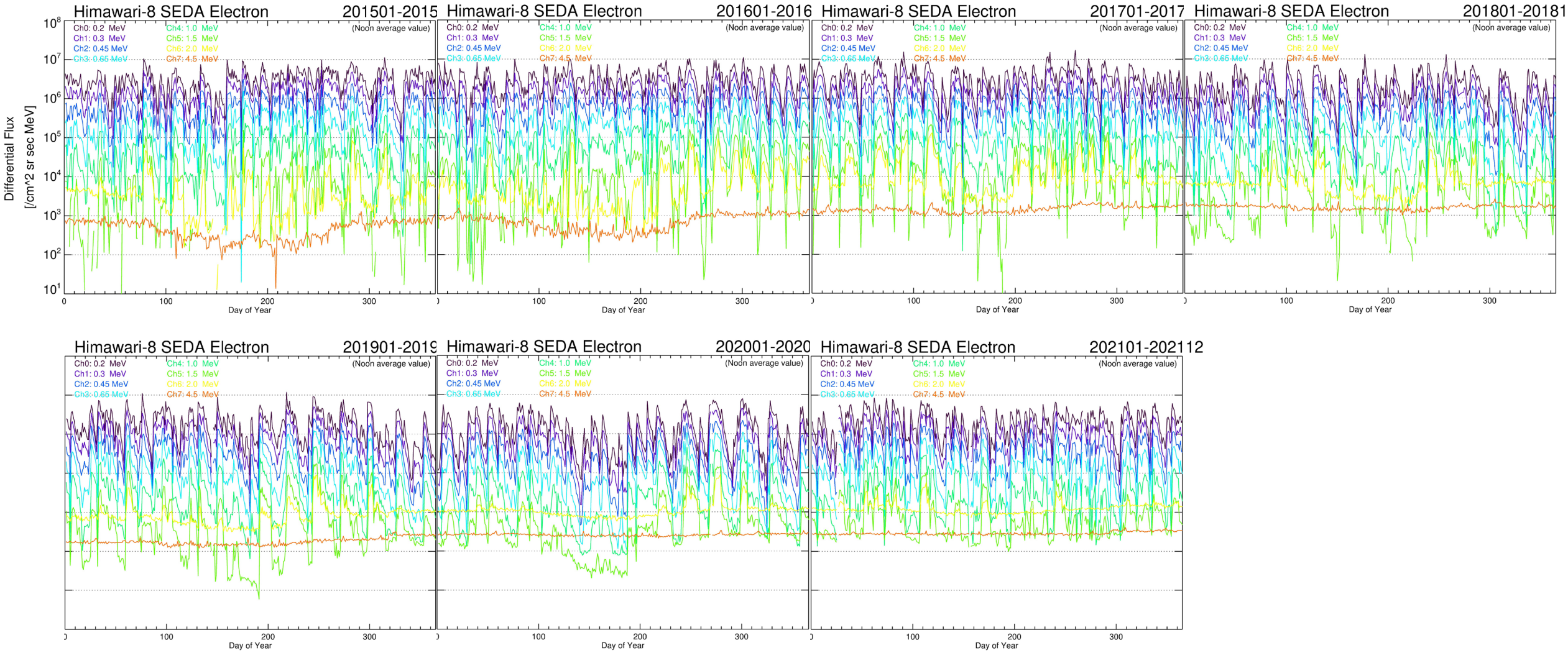

Long-term variations of SEDA-e measurements (2015-2021) Ch.6,7

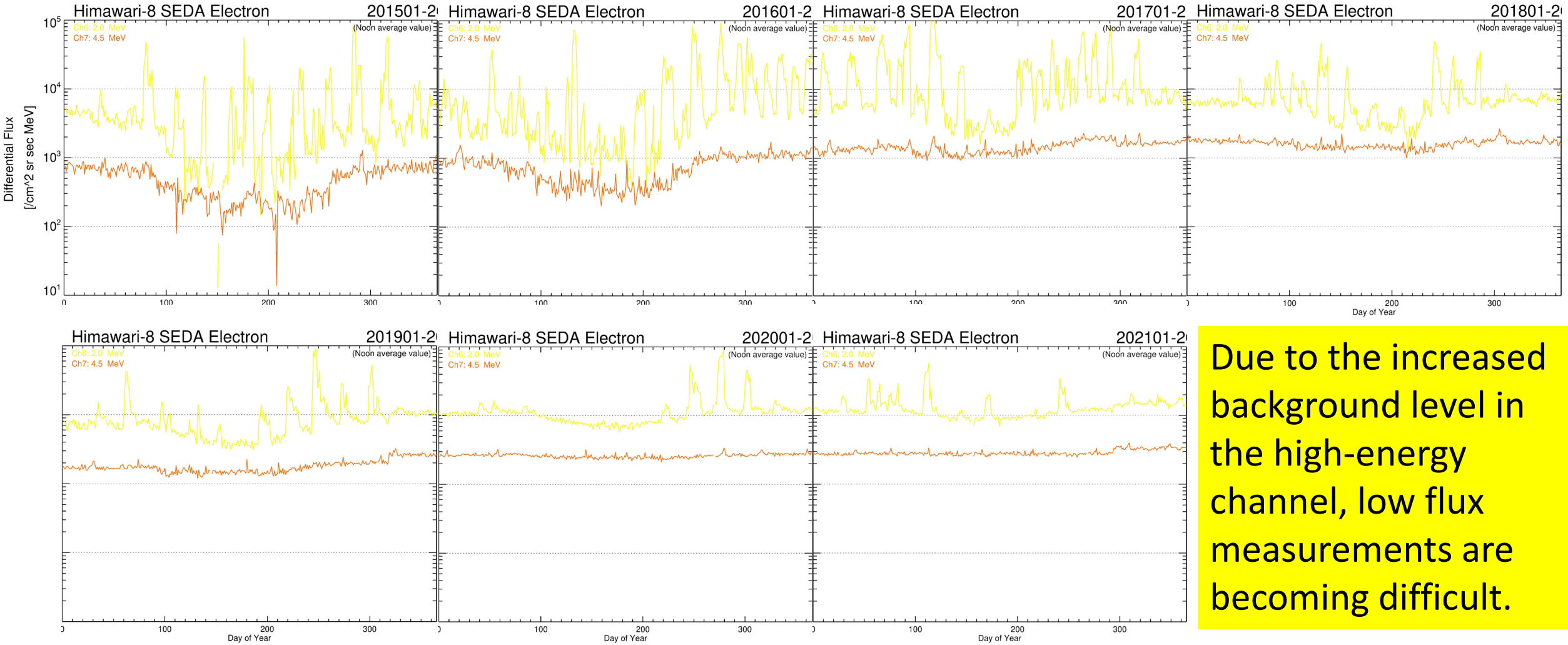

Due to the increased background level in the high-energy channel, low flux measurements are becoming difficult.

Seasonal Variations of background flux level of SEDA-e

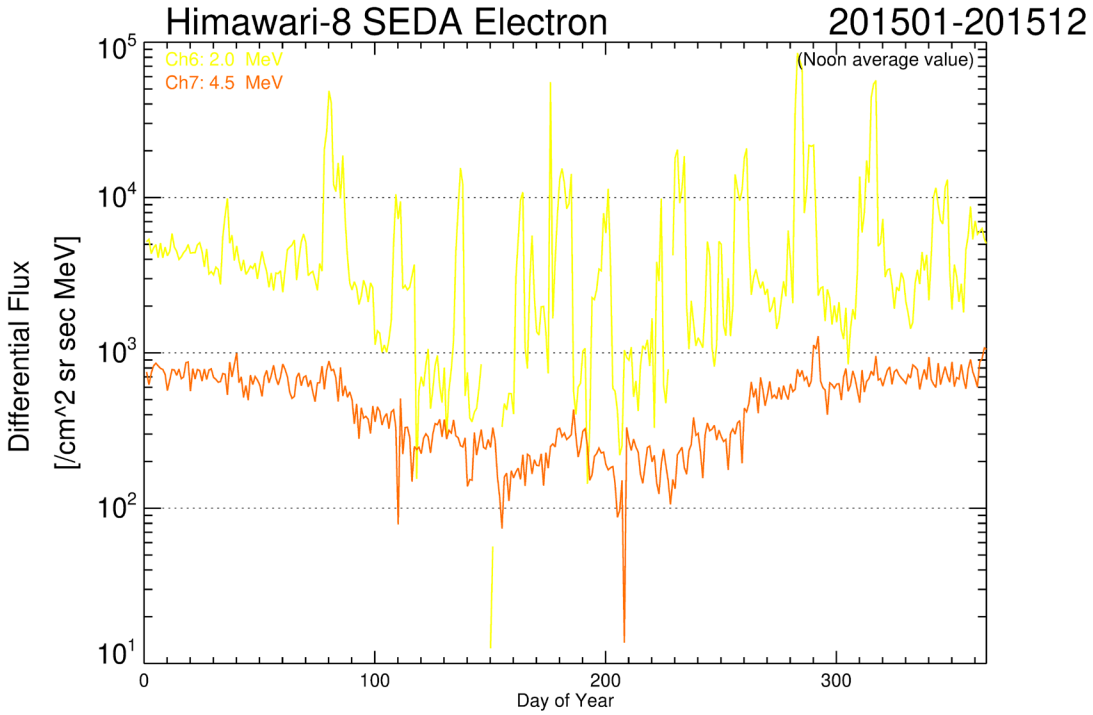

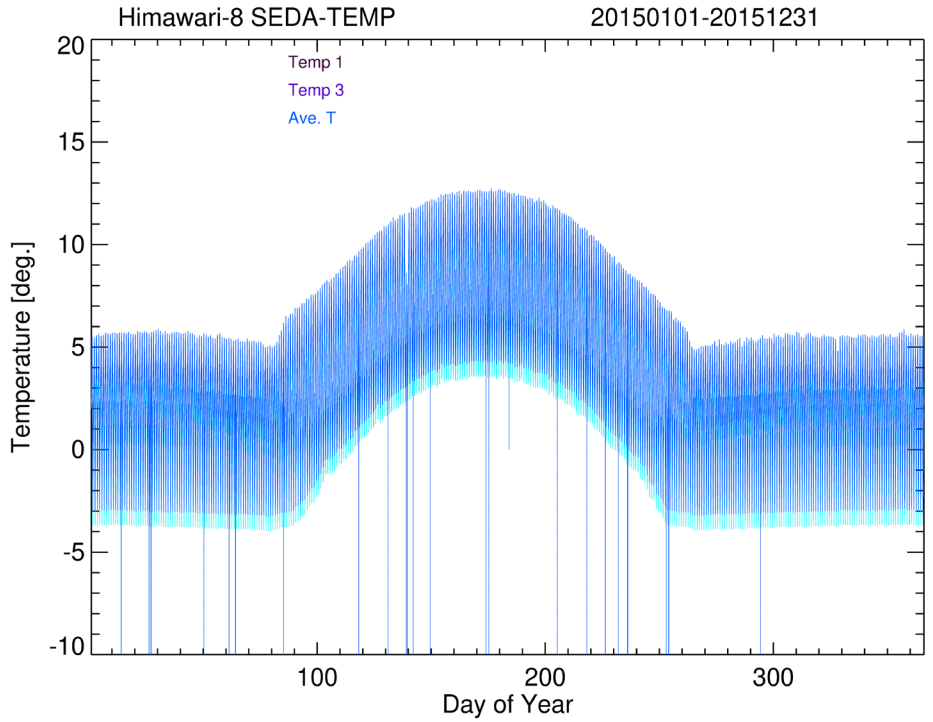

Seasonal variations of background corresponds with those of sensor temperature.

→Effect on residual of bias current subtraction?

Improvement of subtracting bias current

1. Raw data is re-constructed using electron flux data, sensor temperature data, and bias current model derived from ground experiment.
2. Optimized bias current model is estimated from the re-constructed tata.
3. Electron flux data will be improved using new bias current model.

Re-constructed raw data (Ch.0-Ch.3)

Bias current models obtained from ground experiments

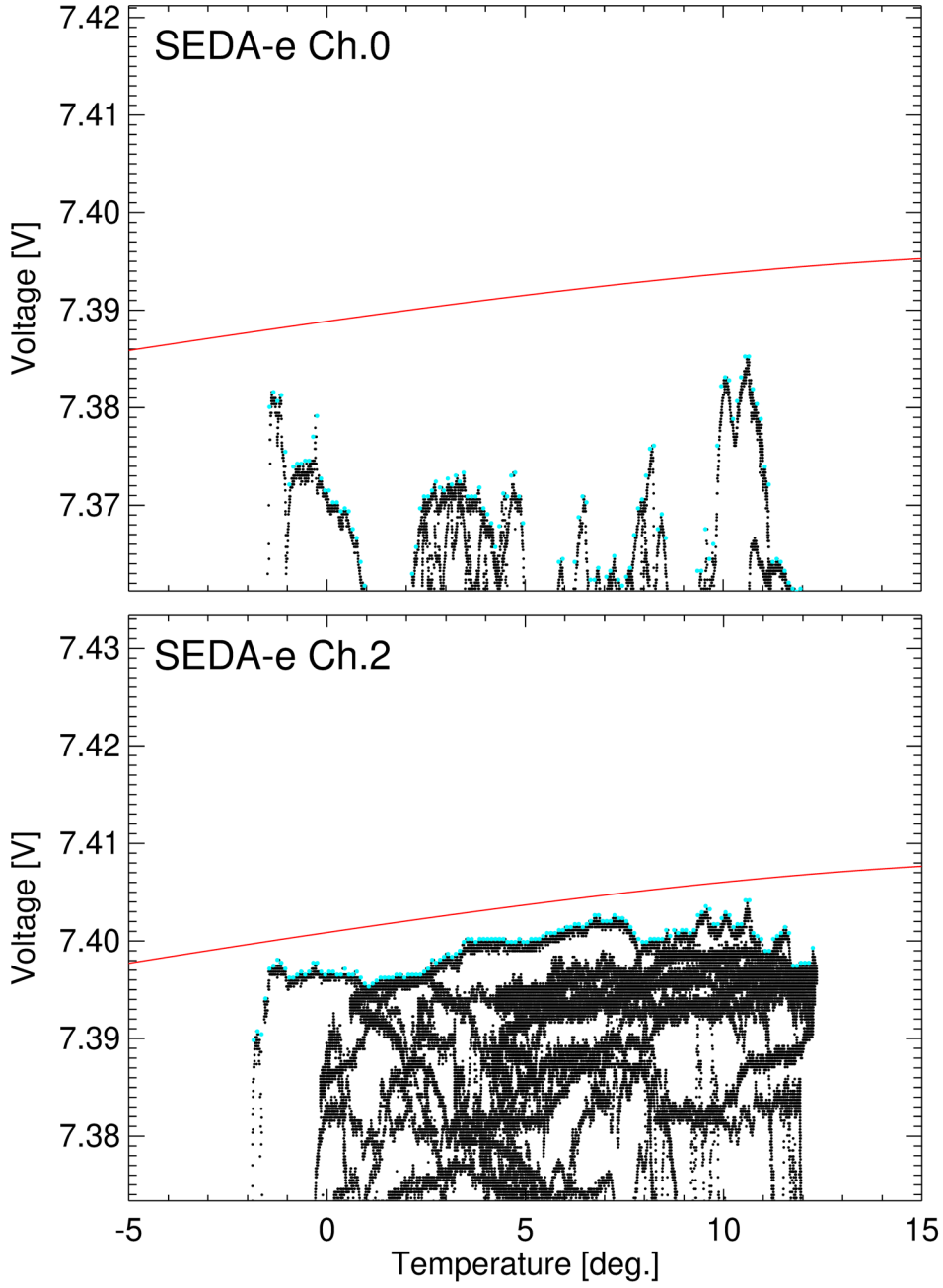

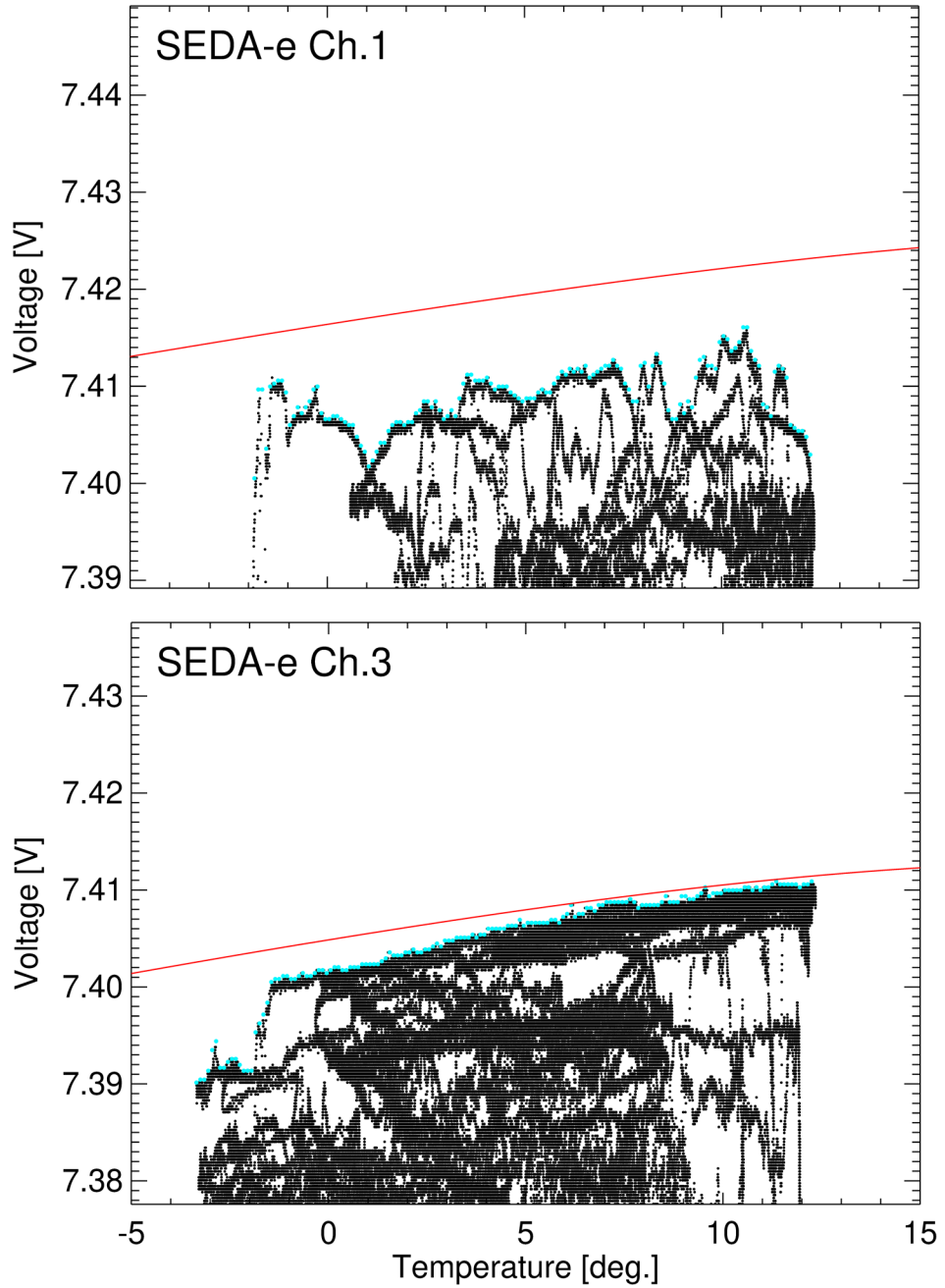

Re-constructed raw data (Ch.4-Ch.7)

Bias current models obtained from ground experiments

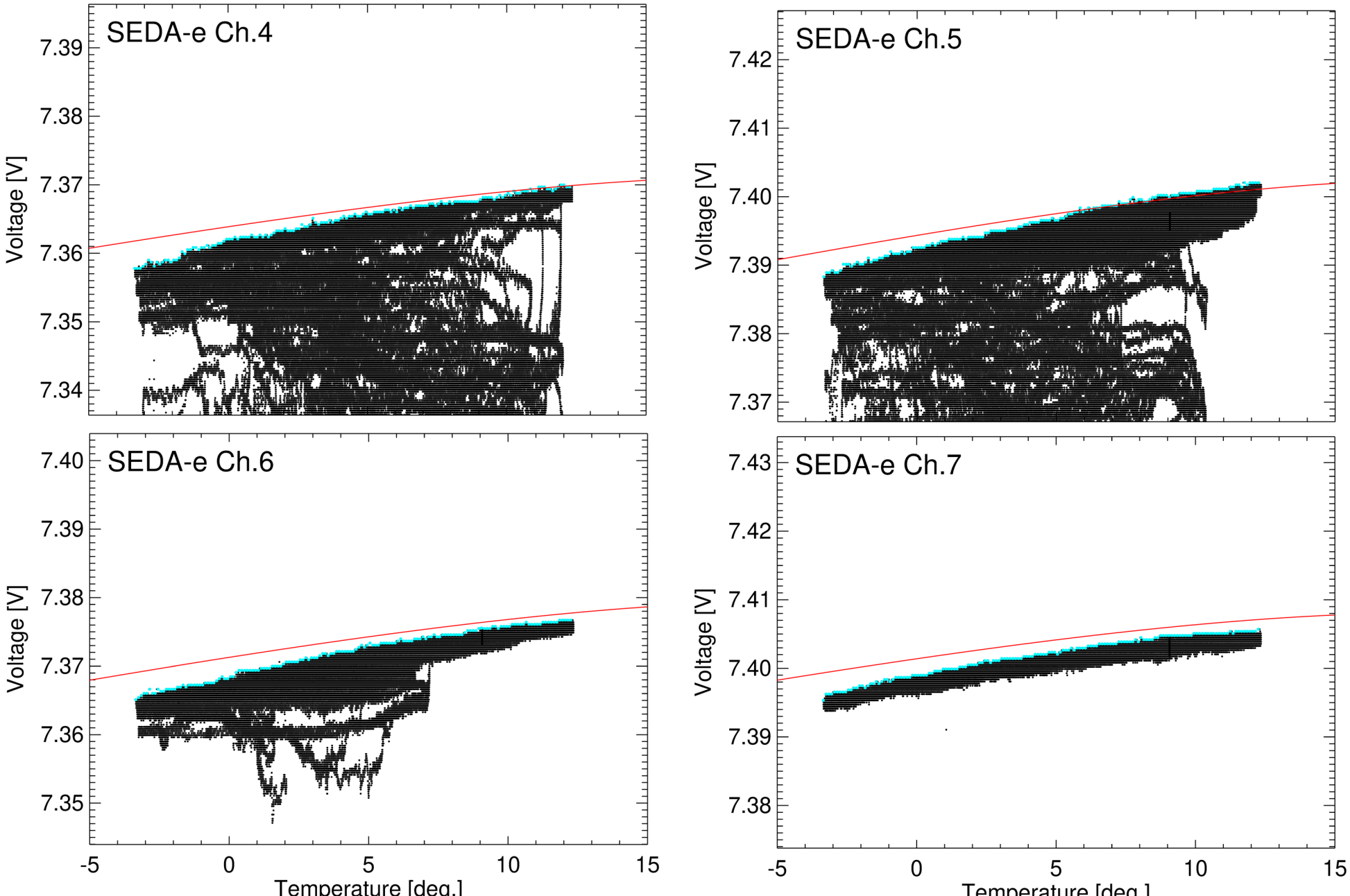

New bias current models (blue lines) [Ch.4-7 only]

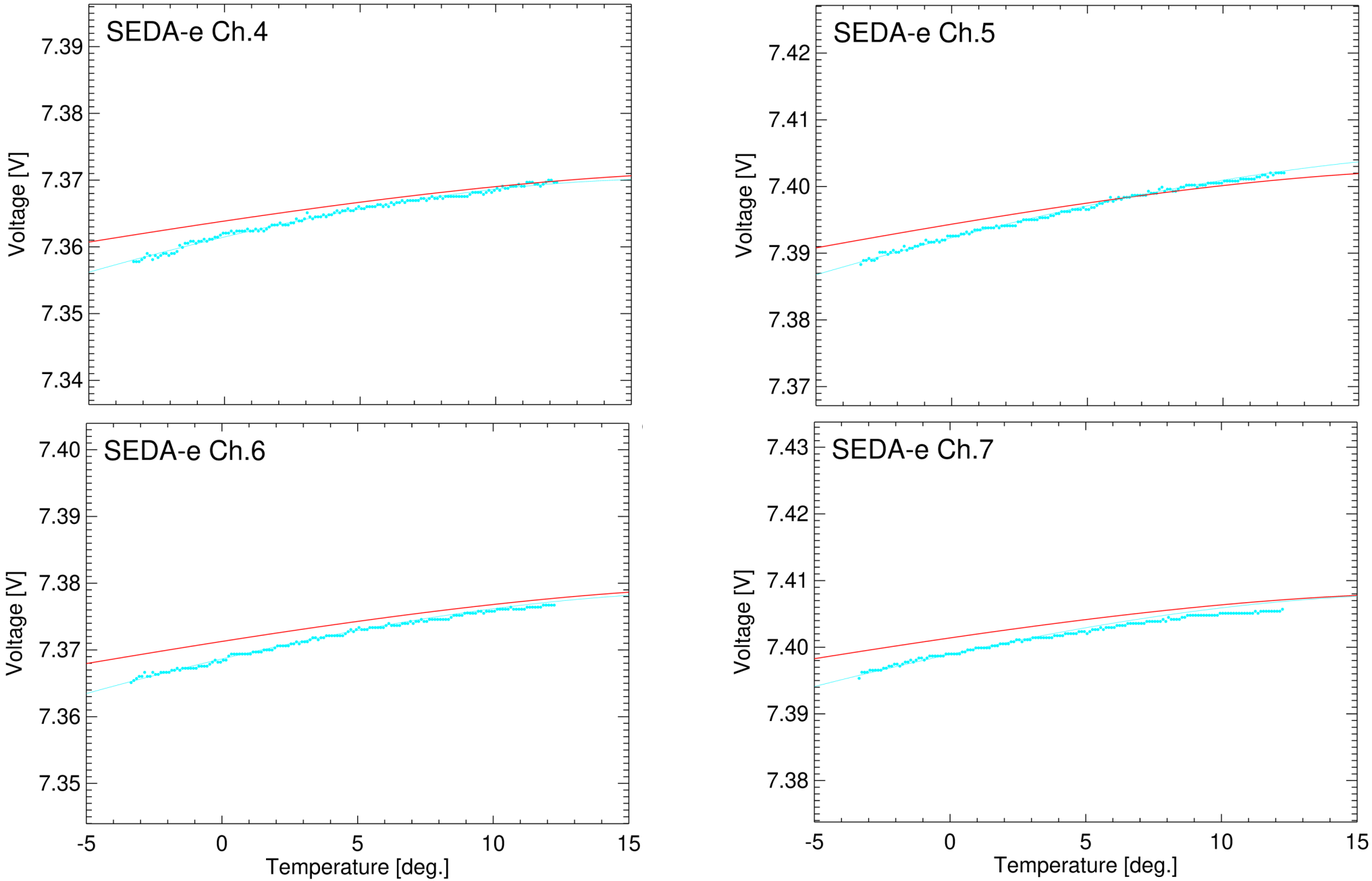

The results of improved bias current subtraction

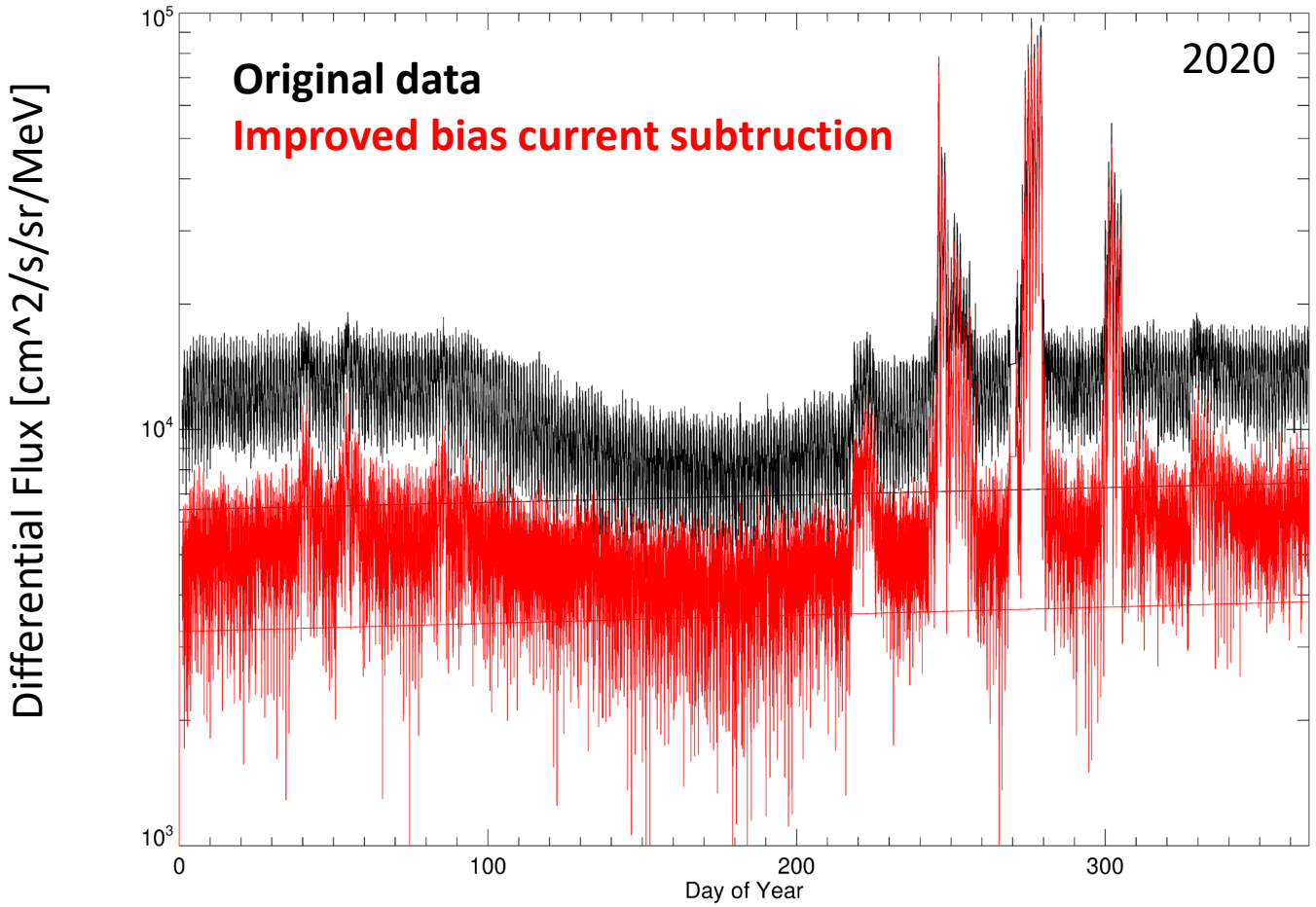

Relationship between long-term trend of bias current and total dose

Long term trend of Ch.7 bias current at the sensor temperature is 4 deg.

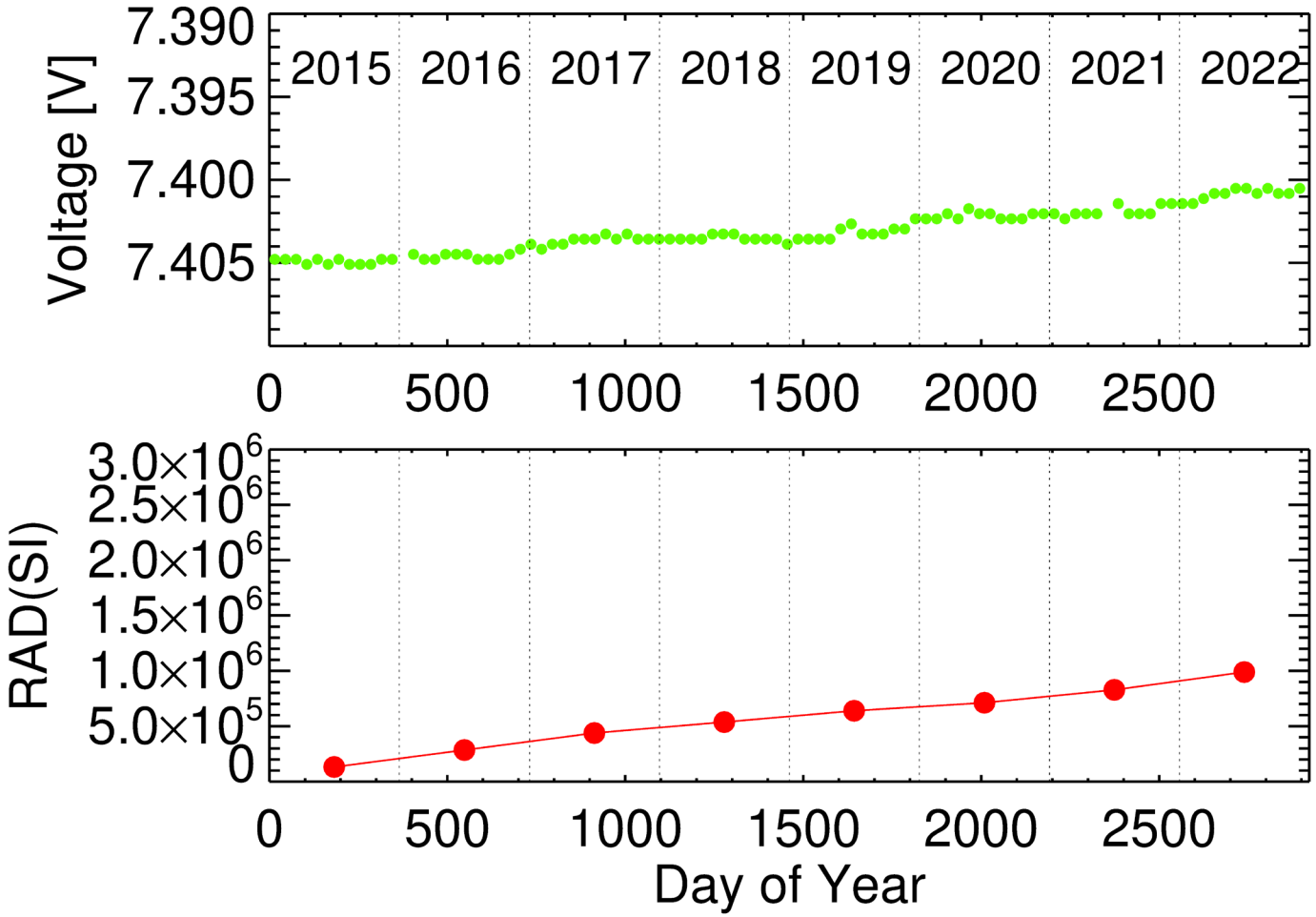

Total does is a possible cause of long-term trend of bias current variation.

Summary

- The bias current of each SEDA-e channel changes over time, and the background flux level in the high-energy channel is increasing year by year.
- The increasing background level can be reduced by improving the bias current model (but only for the high energy channel).
- The total dose effect may be a factor in the change in bias current over time.

Procedure of cross calibration

1. Determination of L* conjunction
2. Interpolation for adjusting energy
3. Flux projected to geomagnetic equator
4. Comparison

Comparison between GOES 16 and Himawari-8

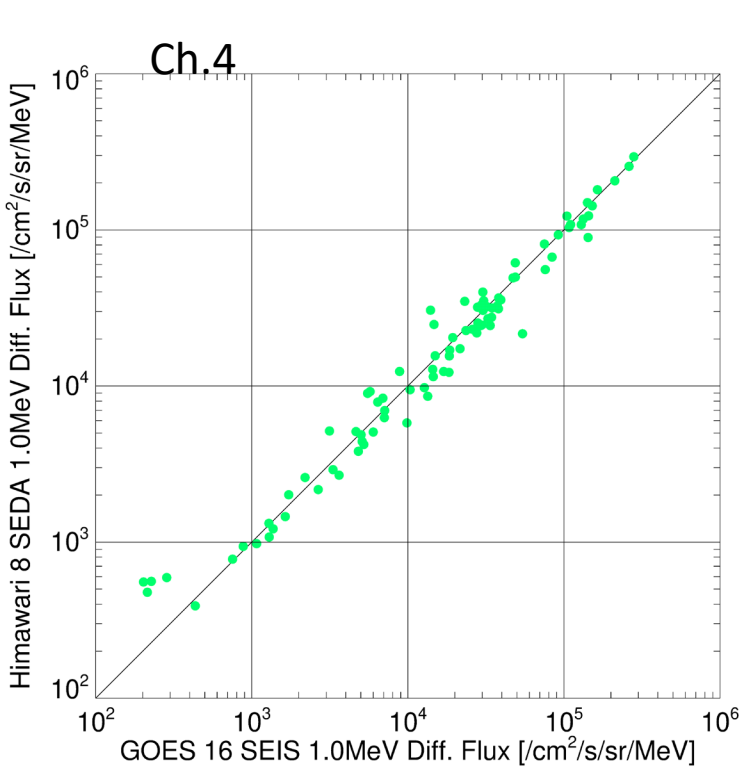

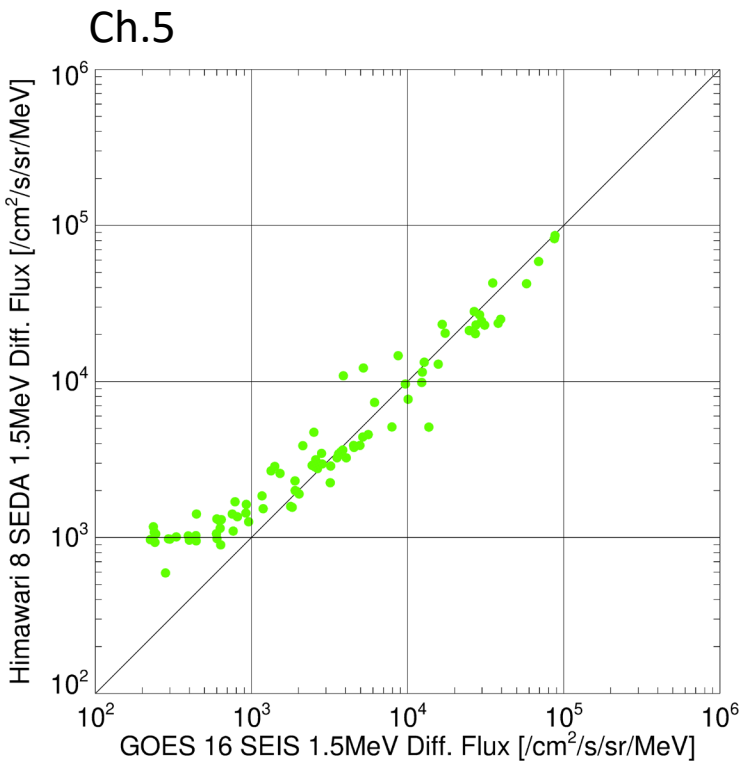

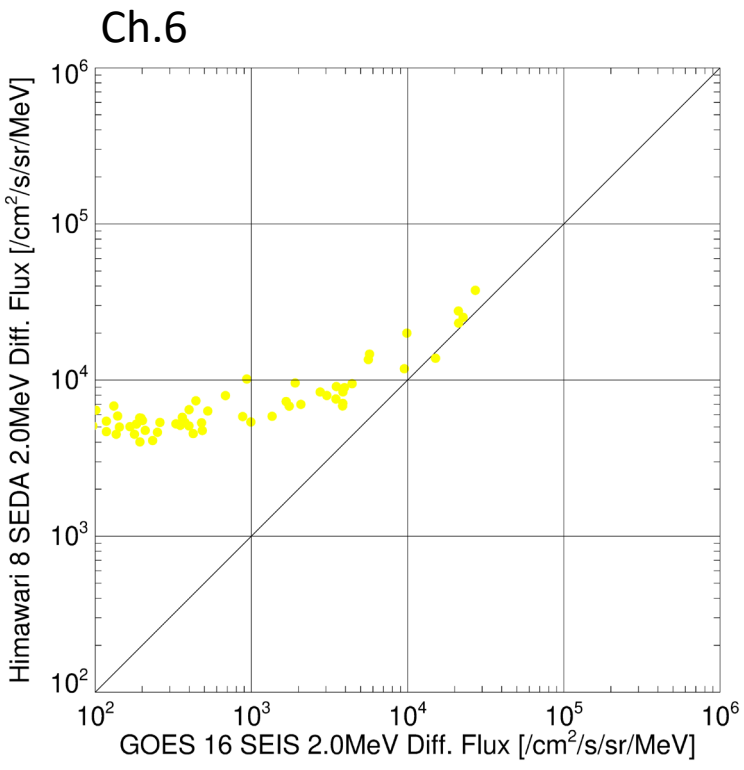

Value of lower flux is improved by using new bias current model.

L* (Roederer's L)

- Indicator of particle drift shell
- If L* is the same, both satellite observes the same drift shell of the particles.
- L* is strongly depend on the magnetospheric model. (We use **Olson-Pfitzer quiet model**.)

$$L^* = -\frac{2\pi k_0}{\Phi R_E} \qquad \Phi = \int \boldsymbol{B} \cdot d\boldsymbol{S}$$

- k_0 : The E omer
- R_E : Radius of the Earth

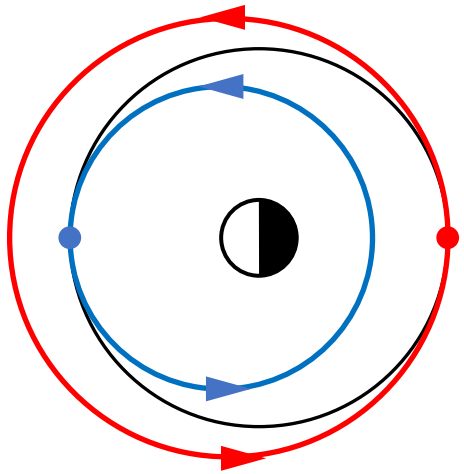

Identify L* conjunction period

- Comparing particle data which observes particles in the same drift shell.
- We should avoid magnetic local time (MLT) around midnight and noon. [Friedel et al., 2005]
- L* is calculated using IRBEM library.

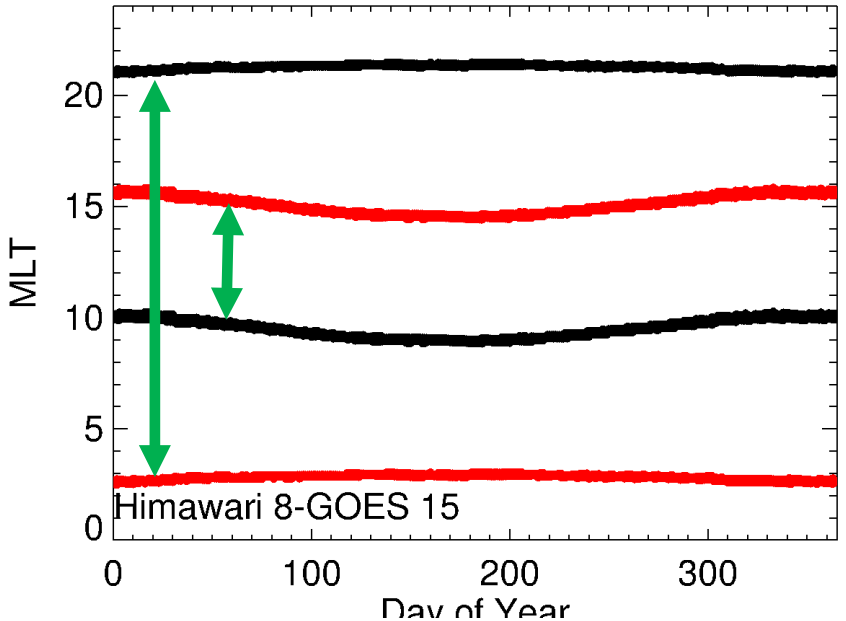

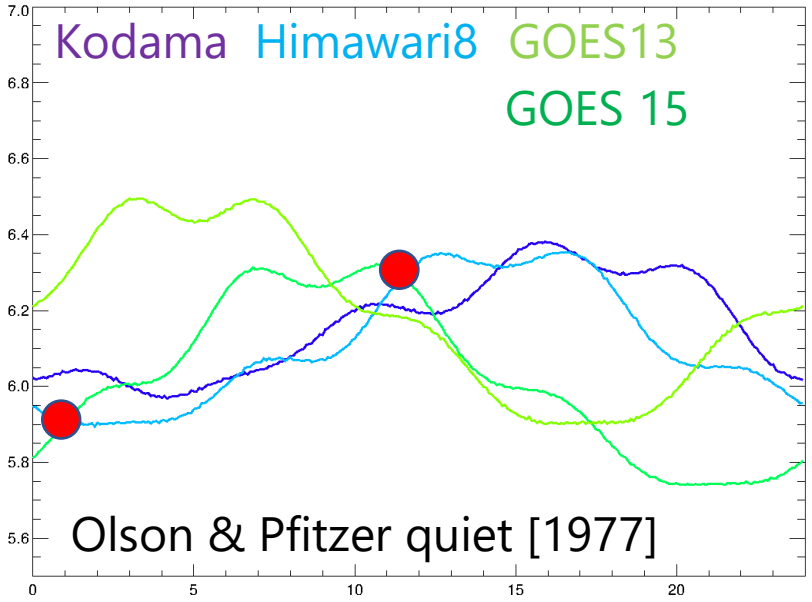

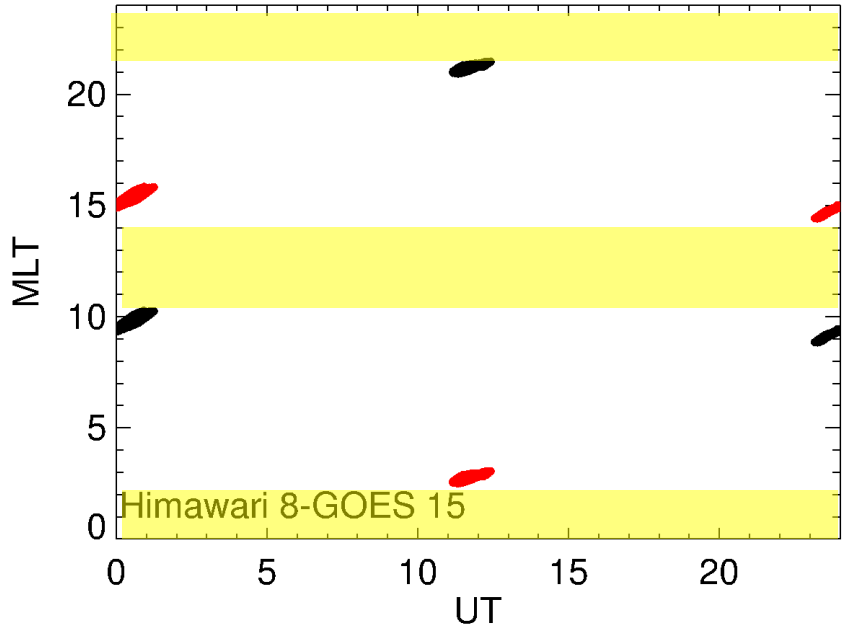

GOES-16 Space Environment in-situ suite (SEISS) Magnetospheric Particle Sensor – High Energy (MPS-HI)

The MPS-HI sensor monitors medium and high energy protons and electrons.

Electron Energy of each channel [keV]

- E1 : 67.7
- E2 : 131.3
- E3 : 183.1
- E4 : 288.6
- E5 : 412.8
- E6 : 600.3
- E7 : 900.3
- E8 : 1493.1
- E9 : 1969.0
- E10: 2907.2

Interpolation of adjusting SEDA-e channels [keV]

- E0: 200 from MPS-HI E3&E4
- E1: 300 from MPS-HI E4&E5
- E2: 450 from MPS-HI E5&E6
- E3: 650 from MPS-HI E6&E7
- E4: 1000 from MPS-HI E7&E8
- E5: 1500 from MPS-HI E8
- E6: 2000 from MPS-HI E9
- E7: 4500

We use log-linear interpolation

Flux projected to geomagnetic equator

$$f_{eq}(E) = f_{\lambda}(E, \alpha_{\lambda}) \left(\frac{B_{\lambda}}{B_{eq}} \right)^{\frac{m}{2}} / sin^{m} \alpha_{\lambda}$$

$$f_{eq}(E) = f_{\lambda}(E) \left(\frac{B_{\lambda}}{B_{eq}} \right)^{\frac{1}{2}} \qquad \text{If m = 1}$$

- We assume isotropic flux distribution.

Comparison between 2017/04-06 and 2020/04-06(1/2)

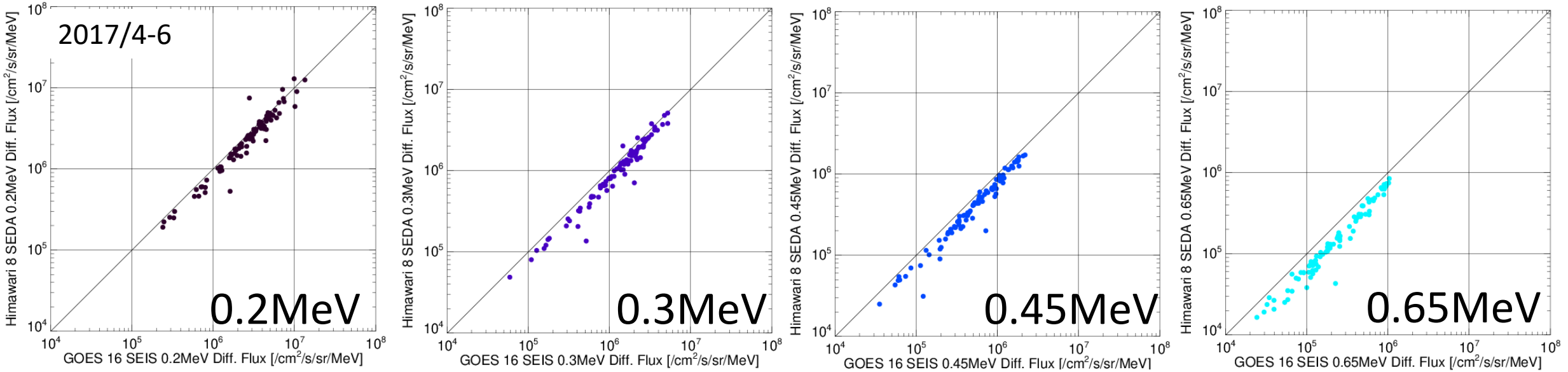

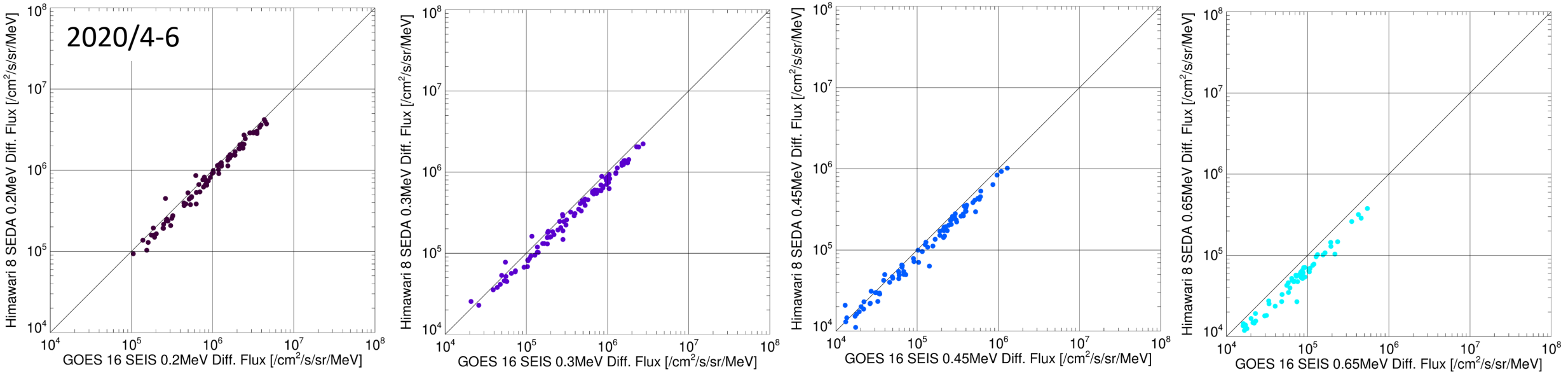

Comparison between 2017/04-06 and 2020/04-06(2/2)

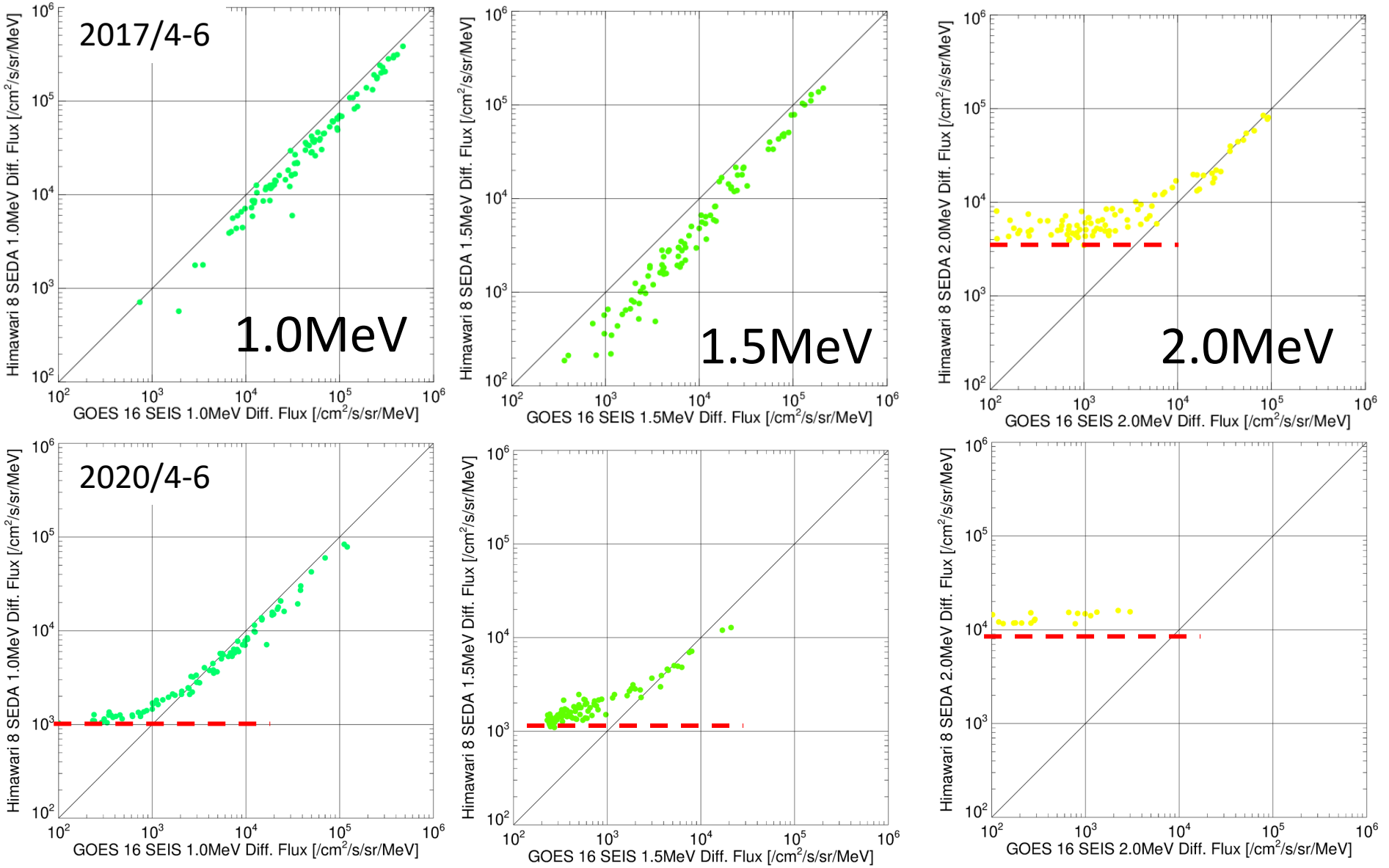

Our initial comparison between Himawari-8 and GOES 16 suggests that

***There is no long-term variation of the sensitivity of each SEDA-e channel.**

***The level of SEDA's background count is increasing in 2020.**

It seems that the increasing bias current produces the enhancement of the background count.

Seasonal dependence

It seems that there is no seasonal dependence for the sensitivities of each SEDA-e channels. On the contrary, the background level of several high energy channels needs to be examined in detail.

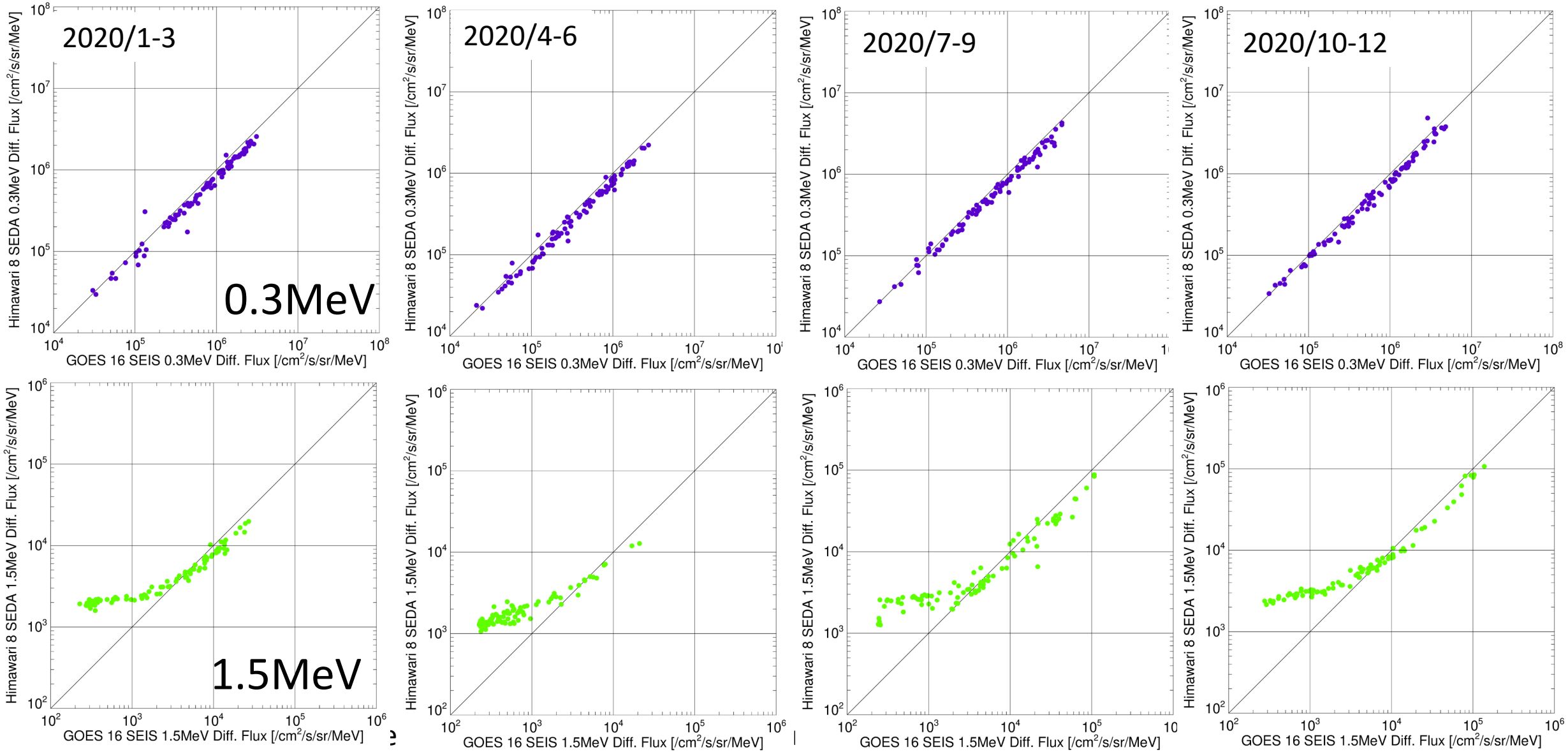

背景：静止軌道の宇宙環境監視の重要性

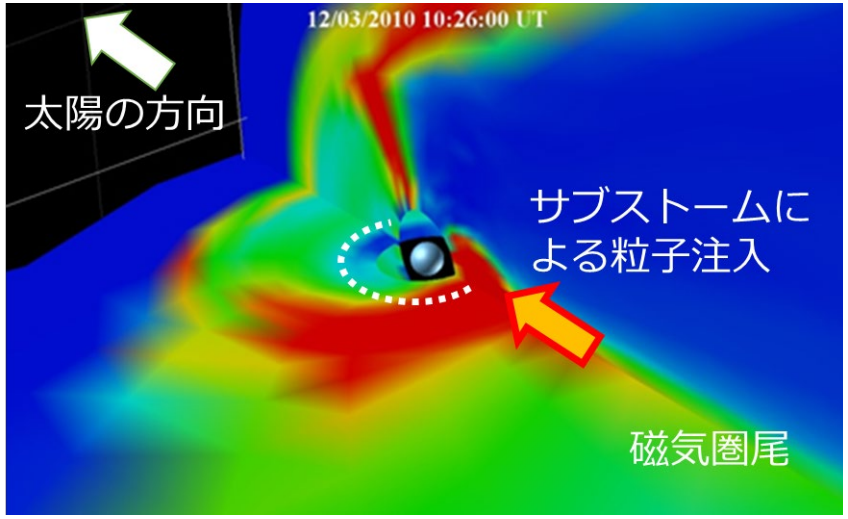

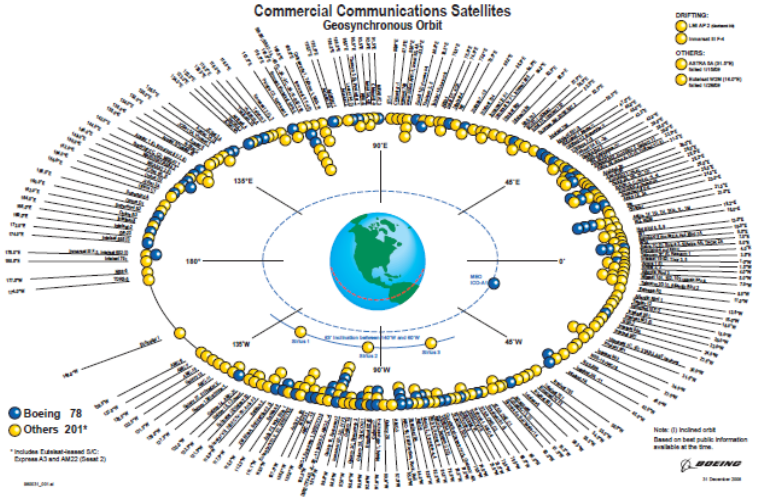

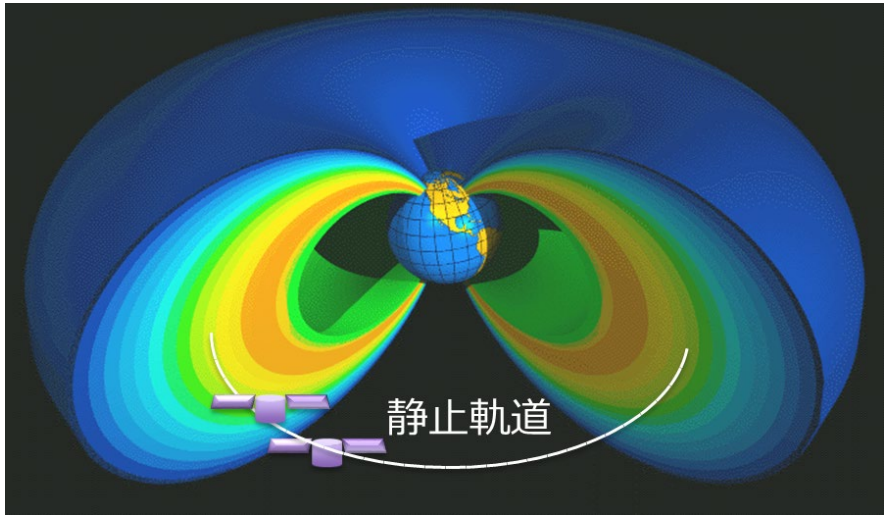

- 静止軌道には現在500機以上の人工衛星が存在しており、通信・放送、気象、測位等様々な実利用に供されている。
- 静止軌道は磁気圏サブストームによって数～数百KeVの電子・イオンのfluxが増大する領域であり（表面帯電の要因）、かつ、放射線帯外帯の外縁部に位置し、地磁気擾乱によって、数百keV以上の電子fluxが増大する領域である（内部帯電の要因）。
- 安心・安全な衛星運用の実現の為に、静止軌道周辺の宇宙環境の監視・予測が重要である。

Coordination Group for Meteorological Satellite（CGMS：気象衛星調整会議）

- 宇宙からの気象観測・宇宙天気観測を実施している機関で構成されるコンソーシアム。WMO等が策定した要件に応じて、気象観測・予測及び気候監視業務を支援する目的で1972年に設立。
- 当初は宇宙からの気象・気候監視のみを取り扱っていたが、WMOが2009年から宇宙天気観測への関与を深めていくのに呼応して、2012年にad-hocな組織として宇宙天気タスクチーム（Space Weather Task Team : SWTT）の設置が勧告され、2013年よりSWTTの下で、CGMSにおける宇宙天気観測がに関する議論が本格化。
- 2018年、宇宙天気調整グループ(Space Weather Coordination Group : SWCG)として常設の組織を設置。

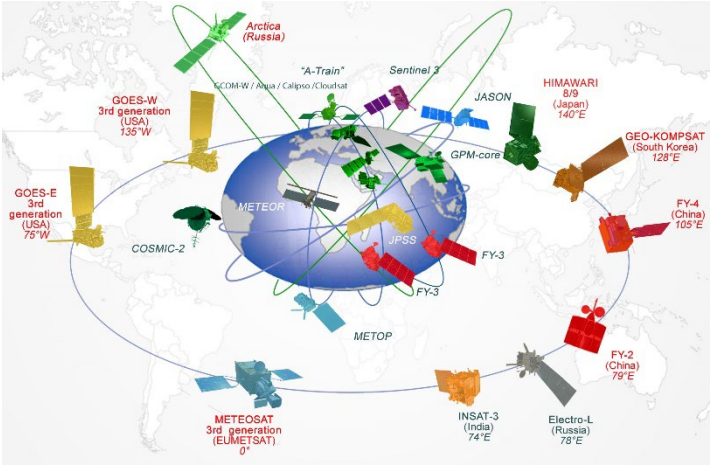

50 YEARS 1972–2022 CGMS

- SWCGでは各機関の宇宙天気計測の現状や将来計画、宇宙天気予報を含むデータ利活用に関する報告や、長期的な宇宙天気観測のギャップ分析とその対応、高エネルギー粒子計測器の相互校正手法の検討や標準化、宇宙天気に起因する衛星障害情報のデータベース化などに関して、他のWGとも連携しながら議論を行っている。